

Bulk viscosity for pion and nucleon thermal fluctuation in the hadron resonance gas model

Sabyasachi Ghosh,^{1,2,*} Sandeep Chatterjee,^{2,3,†} and Bedangdas Mohanty^{2,‡}

¹*Department of Physics, University of Calcutta, 92, A. P. C. Road, Kolkata - 700009, India*

²*School of Physical Sciences, National Institute of Science Education and Research, Jatni, 752050, India*

³*Theoretical Physics Division, Variable Energy Cyclotron Centre, 1/AF, Bidhan Nagar, Kolkata - 700064, India*

We have calculated microscopically bulk viscosity of hadronic matter, where equilibrium thermodynamics for all hadrons in medium are described by Hadron Resonance Gas (HRG) model. Considering pions and nucleons as abundant medium constituents, we have calculated their thermal widths, which inversely control the strength of bulk viscosities for respective components and represent their in-medium scattering probabilities with other mesonic and baryonic resonances, present in the medium. Our calculations show that bulk viscosity increases with both temperature and baryon chemical potential, whereas viscosity to entropy density ratio decreases with temperature and with baryon chemical potential, the ratio increases first and then decreases. The decreasing nature of the ratio with temperature is observed in most of the earlier investigations with few exceptions. We find that the temperature dependence of bulk viscosity crucially depends on the structure of the relaxation time. Along the chemical freeze-out line in nucleus-nucleus collisions with increasing collision energy, bulk viscosity as well as the bulk viscosity to entropy density ratio decreases, which also agrees with earlier references. Our results indicate the picture of a strongly coupled hadronic medium.

PACS numbers: 11.10.Wx, 12.39.Ki

I. INTRODUCTION

The extraction of the transport properties of the strongly interacting medium created in heavy ion collision (HIC) experiments is currently a very active topic of research in the HIC community. The methods of relativistic hydrodynamics with minimal viscous correction have been quite successful in describing the time evolution of the hot and dense fireball created in the HIC experiments. These kind of investigations have also concluded that the shear viscosity (η) to entropy density (s) ratio, η/s , of the medium created in HIC experiments is very close to its quantum lower bound $1/4\pi$ [1]. Similar to η , another transport coefficient is the bulk viscosity, ζ , which is defined as the proportionality constant between the non-zero trace of the viscous stress tensor to the divergence of the fluid velocity, and usually it appears associated with processes accompanied by a change in fluid volume or density. The viscous coefficient ζ has received much less attention than the η in hydrodynamical simulations because its numerical value is assumed to be very small, as it is directly proportional to the trace of the energy-momentum tensor, which generally vanishes for conformally symmetric matter [2]. However, according to Lattice Quantum Chromo Dynamics (LQCD) calculations [3], the trace of the energy momentum tensor of hot QCD medium might be large near the QCD phase transition, which indicates the possibility of a non-zero and

large value of ζ as well as of ζ/s near the transition temperature. This indication is confirmed by the Refs. [4, 5], related with LQCD estimation, where Ref. [5] exposes the possibility of divergence of ζ near the transition temperature. In recent times, different phenomenological investigations [6–18] demonstrated that bulk viscosity can have a non-negligible effect on heavy ion observables, where the values of ζ/s in Ref. [18] is assumed to be quite large.

On the basis of phenomenological importance, microscopic calculations of ζ for quark gluon plasma (QGP) and hadronic matter is a matter of contemporary interest in the community of HIC. A list of references are [2, 19–37], where Ref. [19] addressed high temperature perturbative QCD calculations of ζ , Refs. [20–25] have gone through Nambu-Jona-Lasinio (NJL) model calculations of ζ and Refs. [26–28] provided the discussions on Linear Sigma Model (LSM) estimation of ζ . These effective QCD model calculations [20–28] cover both QGP and hadronic phases while hadronic-model calculations of Refs. [32–37] are restricted within hadronic phase only. The present work is also addressing the estimation of ζ in the hadronic phase only. At vanishing baryonic chemical potential, most of the microscopic calculations predict that $\zeta(T)$ increases but $\zeta/s(T)$ decreases in the hadronic temperature domain. However, few exceptions are there depending on different scenario. For example, Ref. [28] showed that the decreasing function of $\zeta/s(T)$ is transformed to an increasing function in the hadronic temperature domain, when its medium constituents sigma meson becomes heavier. Similar kind of fact is also observed in Ref. [27] depending on the different nature of phase transition as well as methodological differences of LSM calculations. In the hadronic temperature domain, a decreasing nature of $\zeta(T)$ is observed in Ref. [20] while

*Electronic address: sabyaphy@gmail.com

†Electronic address: sandeepc@niser.ac.in

‡Electronic address: bedanga@niser.ac.in

Ref. [33] estimated increasing $\zeta/s(T)$. These knowledge from the earlier investigations suggest that the nature of $\zeta(T)$ and $\zeta/s(T)$ are still not very settled issues. Again, the numerical strength of ζ and ζ/s from different model calculations exhibit a large band - $\zeta \sim 10^{-5} \text{ GeV}^3$ [32] to 10^{-2} GeV^3 [20] or, $\zeta/s \sim 10^{-3}$ [32] to 10^0 [20]. These uncertainty in nature as well as numerical values of $\zeta(T)$ from the earlier investigations demand for further research on these kind of microscopic calculations. Owing to that motivation, we have gone through a microscopic calculations of ζ and ζ/s , where equilibrium situations of hadronic matter are controlled by the standard HRG model and non-equilibrium picture of medium constituents is introduced via quantum fluctuation of pion and nucleon in medium. With respect to the earlier HRG calculations of ζ [33–36], the main distinguishable contribution is in the non-equilibrium properties of medium constituents, quantified by their thermal width. Assuming pions and nucleons as most abundant constituents of medium, we have calculated their thermal width, which are coming from their in-medium scattering with different possible mesonic and baryonic resonances. The main formalism for this thermal width calculations of pion and nucleon are explicitly described in the Section II, which is started with a brief description HRG model, handling the equilibrium part. Next, the numerical results are discussed in Section III and lastly, our investigations have been summarized and concluded in Section IV.

II. FORMALISM

The HRG system is an ideal gas of hadrons and their resonances are taken from the Particle Data Book [38]. Here we consider all resonances up to 2 GeV masses. The recent LQCD data at zero baryon chemical potential (μ_B) show that for temperatures up to the crossover region (150 – 160 MeV), HRG provides a reasonably good description of the LQCD thermodynamics [39–41]. All thermodynamic quantities of the HRG can be computed from the logarithm of total partition function

$$\ln Z_{HRG}(T, \mu_B, \mu_Q, \mu_S) = \sum_i \ln Z_s^i(T, \mu_B, \mu_Q, \mu_S) , \quad (1)$$

where

$$\ln Z_s^i = \frac{g_i}{2\pi^2} VT^3 \sum_{n=1}^{\infty} \frac{(\mp 1)^{(n+1)}}{n^4} \left(\frac{nm_i}{T}\right)^2 K_2\left(\frac{nm_i}{T}\right) e^{n\beta\mu_i} \quad (2)$$

is the single particle partition function of the i th hadron. In Eq. (2), g_i is the degeneracy factor of i th particle with mass m_i , V is volume of the medium, and $K_2(\cdot)$ is the modified Bessel function. Under the condition of complete chemical equilibrium, all the hadron chemical potentials can be expressed in terms of only three chemical potentials corresponding to the QCD conserved charges

$$\mu_i = B_i\mu_B + Q_i\mu_Q + S_i\mu_S \quad (3)$$

where B_i , Q_i and S_i are the baryon number, electric charge and strangeness of the i th hadron. It is straightforward to compute other thermodynamic quantities from Z_{HRG} , such as pressure (P), energy density (ϵ), entropy density (s):

$$P = -\frac{T}{V} \ln Z_{HRG} , \quad (4)$$

$$\epsilon = \frac{1}{V} \left\{ T^2 \frac{\partial \ln Z_{HRG}}{\partial T} + \sum_i \mu_i T \frac{\partial \ln Z_{HRG}}{\partial \mu_i} \right\} , \quad (5)$$

$$s = \frac{1}{T} \left\{ \epsilon + P - \frac{1}{V} \sum_i \mu_i T \frac{\partial \ln Z_{HRG}}{\partial \mu_i} \right\} . \quad (6)$$

Square of the speed of sound is defined as

$$c_s^2 = \left(\frac{\partial P}{\partial \epsilon} \right)_{\rho_B} , \quad (7)$$

where ρ_B is net baryon density.

From the Relaxation Time Approximation (RTA) of kinetic theory approach [28, 31] or from the one-loop expression of diagrammatic approach based on Kubo formula [37], we can get standard expressions of bulk viscosity coefficient for pion and nucleon components [28, 31, 34, 37] :

$$\zeta_\pi = \left(\frac{g_\pi}{T} \right) \int \frac{d^3 \mathbf{k}}{(2\pi)^3} \frac{n_\pi [1 + n_\pi]}{\omega_\pi^2 \Gamma_\pi} \left\{ \left(\frac{1}{3} - c_s^2 \right) \mathbf{k}^2 - c_s^2 m_\pi^2 \right\}^2 \quad (8)$$

and

$$\begin{aligned} \zeta_N = & \left(\frac{g_N}{T} \right) \int \frac{d^3 \mathbf{k}}{(2\pi)^3} \frac{1}{\omega_N^2 \Gamma_N} \left[\left\{ \left(\frac{1}{3} - c_s^2 \right) \mathbf{k}^2 - c_s^2 m_N^2 \right. \right. \\ & \left. \left. - \omega_N \left(\frac{\partial P}{\partial \rho_B} \right)_\epsilon \right\}^2 n_N^+ (1 - n_N^+) + \left\{ \left(\frac{1}{3} - c_s^2 \right) \mathbf{k}^2 \right. \right. \\ & \left. \left. - c_s^2 m_N^2 + \omega_N \left(\frac{\partial P}{\partial \rho_B} \right)_\epsilon \right\}^2 n_N^- (1 - n_N^-) \right] , \quad (9) \end{aligned}$$

where $n_\pi = 1/\{e^{\omega_\pi/T} - 1\}$ is the Bose-Einstein (BE) distribution function of pion with energy $\omega_\pi = \{\mathbf{k}^2 + m_\pi^2\}^{1/2}$, $n_N^\pm = 1/\{e^{(\omega_N \mp \mu_B)/T} + 1\}$ are the Fermi-Dirac (FD) distribution functions of nucleon and anti-nucleon respectively with energy $\omega_N = \{\mathbf{k}^2 + m_N^2\}^{1/2}$ at finite temperature T and baryon chemical potential μ_B . The degeneracy factors of pion and nucleon components are $g_\pi = 3$ and $g_N = 2 \times 2$ respectively. Next, let us come to the important quantities Γ_π and Γ_N of Eq. (8) and (9), which are called thermal widths of pion and nucleon respectively. During propagation in the medium, pion and nucleon may go through different on-shell scattering with other mesonic (M) and baryonic (B) resonances, which can be quantified by their different possible self-energy diagrams. From the imaginary part of their self-energy functions, their respective thermal widths Γ_π and Γ_N can be found. Fig. 1(a) represents pion self-energy with internal lines of pion (π) and other mesonic resonances

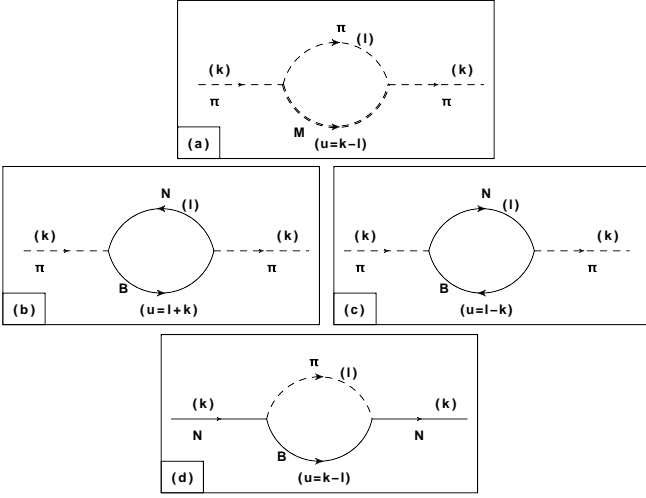


FIG. 1: Pion self-energy diagram with mesonic loops (a) and baryonic loops [(b) and (c) are direct and cross diagrams] and nucleon self-energy diagram (d).

(M), which we can shortly call πM loop. We will take $M = \sigma$ and ρ , as they are dominant resonances of $\pi\pi$ decay channel (within the invariant mass range of 1 GeV). Now, from the retarded self-energy of pion for πM loop $\Pi_{\pi(\pi M)}^R(k)$, the corresponding thermal width $\Gamma_{\pi(\pi M)}$ can be obtained as

$$\Gamma_{\pi(\pi M)} = -\text{Im}\Pi_{\pi(\pi M)}^R(k_0 = \omega_\pi, \vec{k})/m_\pi, \quad (10)$$

where subscript notation stands for external (outside the bracket) and internal (inside the bracket) particles for the diagram 1(a). Following Similar notation, we can define

$$\Gamma_{\pi(NB)} = -\text{Im}\Pi_{\pi(NB)}^R(k_0 = \omega_k^\pi, \vec{k})/m_\pi, \quad (11)$$

where intermediate states of pion self-energy are nucleon N and other baryonic resonance B as shown in Fig. 1(b) along with its cross diagram (c). As a dominant 4-star baryons with spin $J_B = 1/2$ and $3/2$, we have taken $B = \Delta(1232)$, $N^*(1440)$, $N^*(1520)$, $N^*(1535)$, $\Delta^*(1600)$, $\Delta^*(1620)$, $N^*(1650)$, $\Delta^*(1700)$, $N^*(1700)$, $N^*(1710)$ and $N^*(1720)$. Adding all these mesonic (πM) and baryonic (NB) loops, the total thermal width of pion Γ_π can be obtained as

$$\Gamma_\pi = \Gamma_\pi^M + \Gamma_\pi^B = \sum_M \Gamma_{\pi(\pi M)} + \sum_B \Gamma_{\pi(NB)}. \quad (12)$$

Similarly, one-loop self-energy of nucleon with pion (π) and baryon (B) intermediate states, which is denoted as $\Sigma_{N(\pi B)}^R$ (retarded part), will be our matter of interest to estimate corresponding nucleon thermal width $\Gamma_{N(\pi B)}$. The diagrammatic anatomy of $\Sigma_{N(\pi B)}^R$ is shown in Fig. 1(d). Here we have taken all the 4-star spin 1/2 and 3/2 baryons, mentioned above. Hence, summing all the πB loops, we can get our total nucleon thermal width :

$$\Gamma_N = \sum_B \Gamma_{N(\pi B)} = -\sum_B \text{Im}\Sigma_{N(\pi B)}^R(k_0 = \omega_N, \vec{k}). \quad (13)$$

The imaginary part of self-energies, given in Eqs (10), (11) and (13), have been derived with help of standard thermal field theoretical techniques. At first, the expression for $\text{Im}\Pi_{\pi(\pi M)}^R$ is [42]

$$\begin{aligned} \text{Im}\Pi_{\pi(\pi M)}^R(k_0 = \omega_\pi, \vec{k}) &= \int \frac{d^3\vec{l}}{32\pi^2\omega_l\omega_u} \\ &L_{\pi\pi M}(k, l)|_{(l_0=-\omega_l, k_0=\omega_k)} \\ &(n_l - n_u) \delta(\omega_\pi + \omega_l - \omega_u), \end{aligned} \quad (14)$$

where n_l , n_u are BE distribution functions of π , M mesons respectively at energies $\omega_l = \{\vec{l}^2 + m_\pi^2\}^{1/2}$ and $\omega_u = \{\vec{k} - \vec{l}\}^2 + m_M^2\}^{1/2}$. The vertex factors $L_{\pi(\pi M)}(k, l)$ [42] have been calculated by using the effective Lagrangian density,

$$\mathcal{L}_{\pi\pi M} = g_\rho \vec{\rho}_\mu \cdot \vec{\pi} \times \partial^\mu \vec{\pi} + \frac{g_\sigma}{2} m_\sigma \vec{\pi} \cdot \vec{\pi} \sigma, \quad (15)$$

where g_ρ and g_σ are respectively effective coupling constants of ρ meson field ($\vec{\rho}_\mu$) and σ meson field (σ), which are coupled with the pion field ($\vec{\pi}$).

Next, the direct and cross diagrams of pion self-energy for NB loop are combinedly expressed as [44, 45]

$$\begin{aligned} \text{Im}\Pi_{\pi(NB)}^R(k_0 = \omega_\pi, \vec{k}) &= \int \frac{d^3\vec{l}}{32\pi^2\omega_l\omega_u} \\ &L_{\pi NB}(k, l)|_{(l_0=-\omega_l, k_0=\omega_k)} \\ &\{(-n_l^+ + n_u^+) \delta(\omega_\pi + \omega_l - \omega_u) \\ &+ (-n_l^- + n_u^-) \delta(\omega_\pi - \omega_l + \omega_u)\}, \end{aligned} \quad (16)$$

where n_l^\pm , n_u^\pm are FD distribution functions of N and B (\pm for particle and anti-particle) respectively at energies $\omega_l = \{\vec{l}^2 + m_N^2\}^{1/2}$ and $\omega_u = \{\vec{k} \pm \vec{l}\}^2 + m_B^2\}^{1/2}$ (\pm for diagrams (b) and (c) respectively). With the help of the effective Lagrangian densities for πNB interactions [43],

$$\begin{aligned} \mathcal{L}_{\pi NB} &= \frac{f}{m_\pi} \bar{\psi}_B \gamma^\mu \left\{ \frac{i\gamma^5}{\mathbb{1}} \right\} \psi_N \partial_\mu \pi + \text{h.c. for } J_B^P = \frac{1}{2}^\pm, \\ &= \frac{f}{m_\pi} \bar{\psi}_B^\mu \left\{ i\gamma^5 \right\} \psi_N \partial_\mu \pi + \text{h.c. for } J_B^P = \frac{3}{2}^\pm, \\ &(P \text{ stands for parity of } B) \end{aligned} \quad (17)$$

one can deduced the vertex factors $L_{\pi NB}(k, l)$ [44, 45]. At last, the expression for $\text{Im}\Pi_{N(\pi B)}^R$ is [46, 47]

$$\begin{aligned} \text{Im}\Pi_{N(\pi B)}^R(k_0 = \omega_\pi, \vec{k}) &= \int \frac{d^3\vec{l}}{32\pi^2\omega_l\omega_u} \\ &L_{\pi NB}(k, l)|_{(l_0=-\omega_l, k_0=\omega_k)} \\ &(n_l + n_u^+) \delta(\omega_\pi + \omega_l - \omega_u), \end{aligned} \quad (18)$$

where n_l is BE distribution functions of π at energy $\omega_l = \{\vec{l}^2 + m_\pi^2\}^{1/2}$ and n_u^+ is FD distribution of B at energy

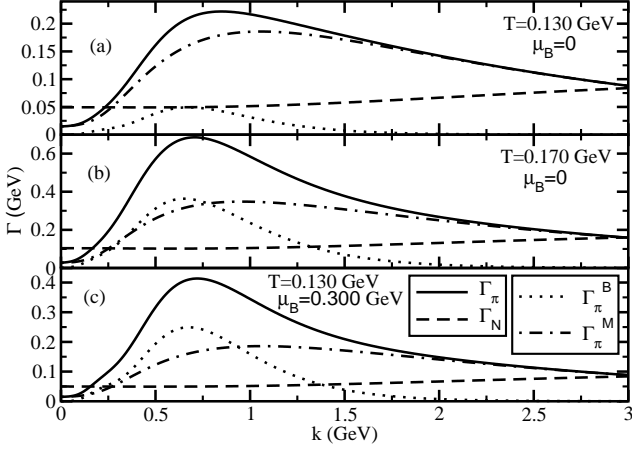


FIG. 2: Momentum distribution of pion thermal width for mesonic (dash-dotted line), baryonic loops (dotted line) and their total (solid line) and nucleon thermal width (dashed line) at three different medium parameters: (a) $(T, \mu_B) = (0.130 \text{ GeV}, 0)$, (b) $(0.170 \text{ GeV}, 0)$ and (c) $(0.130 \text{ GeV}, 0.300 \text{ GeV})$.

$\omega_u = \{(\vec{k} - \vec{l})^2 + m_M^2\}^{1/2}$. With the help of the interaction Lagrangian densities from Eq. (17), the vertex factors $L_{N\pi B}(k, l)$ [46] have been obtained.

III. RESULTS AND DISCUSSION

Let us start our numerical discussion with the Fig. (2), where momentum distribution of thermal widths of pion and nucleon have been displayed. With the help of Eqs. (10), (11), (12), (14) and (16), Γ_π^M , Γ_π^B and their total Γ_π can be found whose momentum distributions are respectively shown by dash-dotted, dotted and solid line in the Fig. (2). Similarly, Γ_N can be deduced by using Eqs. (18) and (13) and its momentum distribution is represented by dash line. Panels (a), (b) and (c) of Fig. (2) are for different set of temperature T and baryon chemical potential μ_B of the medium. Though Γ_N is approximately constant with nucleon momentum, but Γ_π^M and Γ_π^B exhibit a peak structure in some point of \vec{k} -axis, which depends on the medium parameters T and μ_B . These momentum distribution of Γ_π and Γ_N will be integrated out when we will estimate ζ_π and ζ_N from Eqs.(8) and (9) respectively.

Let us come to the different loop contributions of pion and nucleon thermal width in bulk viscosity coefficient of hadronic matter. Fig. 3(c) shows individual contributions of $\pi\sigma$ (dotted line) and $\pi\rho$ (dash line) loops in ζ_π , which reveals that they are respectively important in low ($T < 0.080 \text{ GeV}$) and high ($T > 0.080 \text{ GeV}$) temperature domain for getting a non-divergent values of ζ_π . These are respectively obtained by putting $\Gamma_{\pi(\pi\sigma)}$ and $\Gamma_{\pi(\pi\rho)}$ in place of Γ_π of Eq. (8). Putting $\Gamma_\pi^M = \Gamma_{\pi(\pi\sigma)} + \Gamma_{\pi(\pi\rho)}$ in place of Γ_π of Eq. (8), we get the solid line, repre-

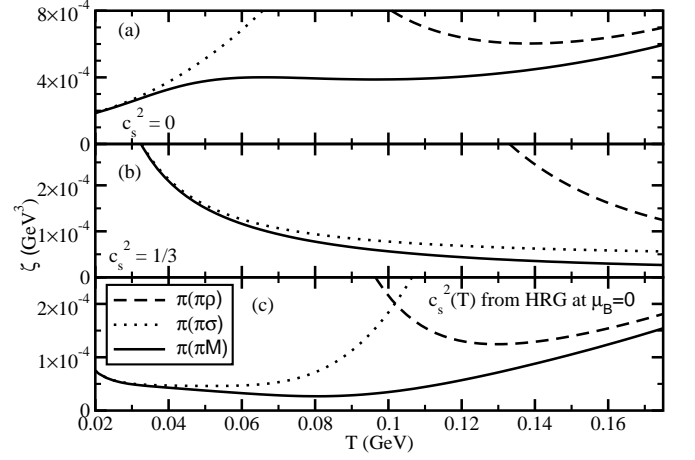


FIG. 3: $\zeta(T)$ due to pion thermal width for $\pi\sigma$ (dotted line), $\pi\rho$ (dashed line) loops and their total (solid line) at $c_s^2 = 0$ (a), $c_s^2 = 1/3$ (b) and $c_s^2(T)$ from HRG (c).

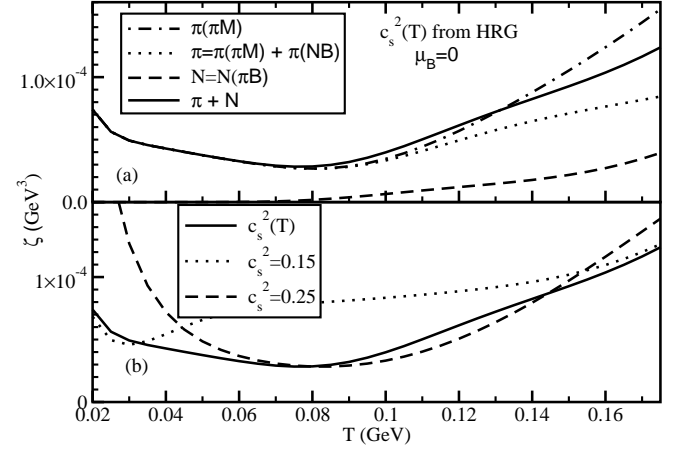


FIG. 4: (a): Temperature dependence of bulk viscosity for pion thermal width with mesonic loops (dash-dotted line), meson + baryon loops (dotted line), for nucleon thermal width (dashed line) and their total $\zeta_T = \zeta_\pi + \zeta_N$ (solid line). (b): $\zeta(T)$ for $c_s^2(T)$ from HRG and two constant values of c_s^2 ($c_s^2 = 0.15$: dotted line and $c_s^2 = 0.25$: dash line).

senting total bulk viscosity of pionic component due to meson loops. After a mild decrement in low T ($< 0.080 \text{ GeV}$), it receives an increment nature in high T ($> 0.080 \text{ GeV}$). Along with Fig. 3(c), where an explicit temperature dependent c_s^2 is taken from HRG model, the results for $c_s^2 = 0$ and $c_s^2 = 1/3$ are also displayed in Fig. 3(a) and (b), which are little different in nature. Just to show the phase space sensitivity of bulk viscosity via c_s^2 , these two results are displaying two extreme limits of c_s^2 . Therefore, we can understand Fig. 3(c) as some sort of superposition of 3(a) and (b).

According to Eq. (12) different baryon loops contribution (Γ_π^B) should have to add with meson loops con-

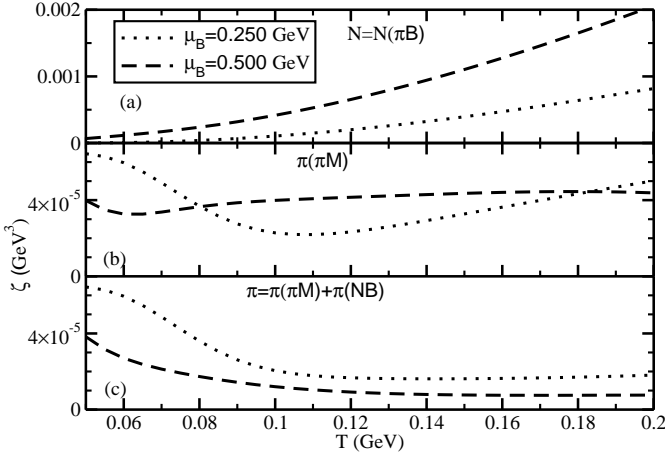


FIG. 5: $\zeta(T)$ due to nucleon thermal width (a), pion thermal width for meson loops (b) and meson + baryon loops (c) at $\mu_B = 0.250$ GeV (dotted line) and 0.500 GeV (dash line).

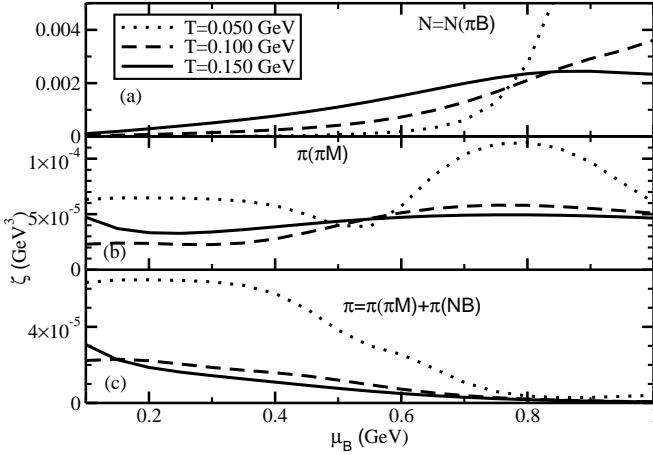


FIG. 6: Same as Fig. (5) along μ_B -axis at $T = 0.050$ GeV (dotted line), 0.100 GeV (dash line) and 0.150 GeV (solid line).

tribution (Γ_π^M) to get total pion thermal width Γ_π . In Fig. 4(a), changing the nature of dash-dotted line to dotted line indicates that inclusion of baryon loops with meson loops becomes the reason for reducing the rate of increment of $\zeta_\pi(T)$ at high temperature region, $T > 0.100$ GeV. Putting our calculated nucleon thermal width Γ_N in Eq. (9), we get ζ_N as shown by dash line in Fig. 4(a). Now adding ζ_N with ζ_π we have total bulk viscosity

$$\zeta_T = \zeta_\pi + \zeta_N, \quad (19)$$

as shown by solid line in Fig. 4(a). In Fig. 4(b), this ζ_T (solid line) has been compared with the results generated for two constant values of c_s^2 ($c_s^2 = 0.25$: dash line and $c_s^2 = 0.15$: dotted line), within which $c_s^2(T, \mu_B = 0)$ from HRG model more or less varies.

At two different values of μ_B , $\zeta(T)$ due to nucleon

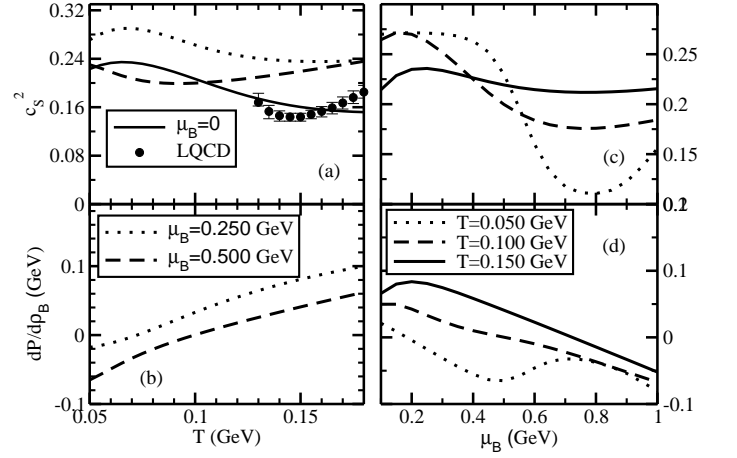


FIG. 7: (a): $c_s^2(T)$ at $\mu_B = 0$ (solid line), 0.250 GeV (dotted line) and 0.500 GeV (dash line), and LQCD results of $c_s^2(T, \mu_B = 0)$ (circles) [3]; (b): $\left(\frac{\partial P}{\partial \rho_B}\right)_\epsilon$ vs T at $\mu_B = 0.250$ GeV (dotted line) and 0.500 GeV (dash line); (c): $c_s^2(\mu_B)$ at $T = 0.050$ GeV (dotted line), 0.100 GeV (dash line) and 0.150 GeV (solid line); (d): $\left(\frac{\partial P}{\partial \rho_B}\right)_\epsilon$ vs μ_B at $T = 0.050$ GeV (dotted line), 0.100 GeV (dash line) and 0.150 GeV (solid line).

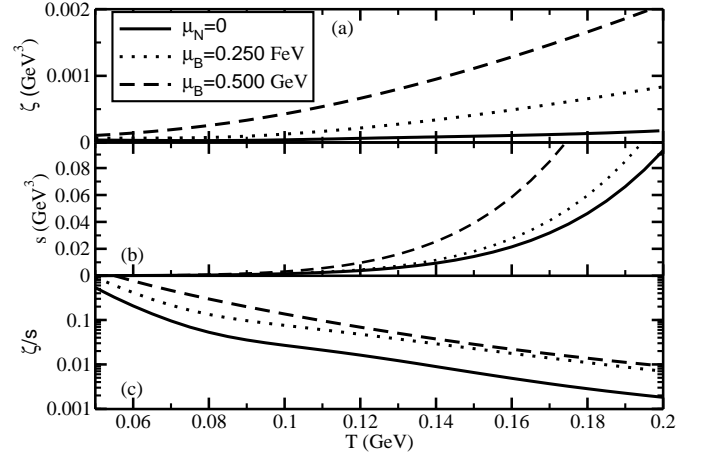


FIG. 8: T dependence of total bulk viscosities (a), entropy densities from HRG (b) and their ratios ζ/s (c) at $\mu_B = 0$ (solid line), 0.250 GeV (dotted line) and 0.500 GeV (dash line).

thermal width (Γ_N), pion thermal width for meson loops (Γ_π^M) and meson + baryon loops (Γ_π) are shown in Fig. 5(a), (b) and (c) respectively. Similarly, Fig. 6(a), (b) and (c) are displaying different loop contributions in $\zeta(\mu_B)$ at $T = 0.050$ GeV (dotted line), 0.100 GeV (dashed line) and 0.150 GeV (solid line). From Fig. 5(a) and 6(a), we see that ζ_N increases with T as well as μ_B . From Fig. 5(b), we see the ζ_π due to Γ_π^M at finite μ_B first decreases at low T then increases at high T . The nature

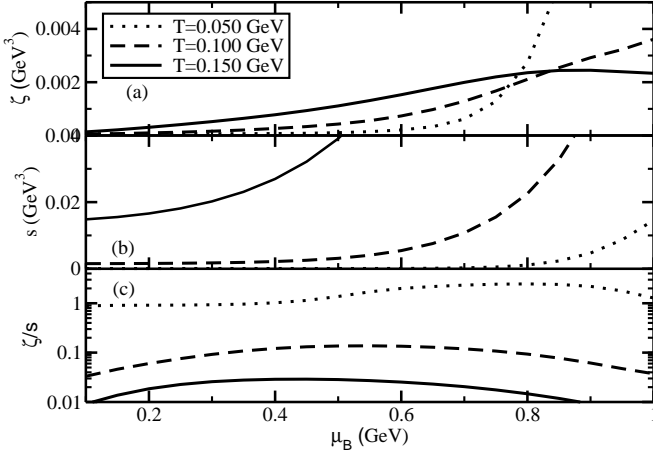


FIG. 9: μ_B dependence of total bulk viscosities (a), entropy densities from HRG (b) and their ratios ζ/s (c) at $T = 0.050$ GeV (dotted line), 0.100 GeV (dash line) and 0.150 GeV (solid line).

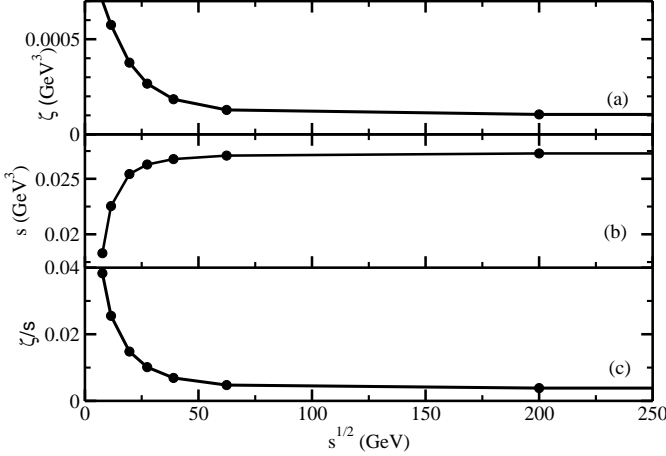


FIG. 10: Center of mass energy (\sqrt{s}) dependence of total bulk viscosity (a), entropy density from HRG (b) and their ratio ζ/s (c).

of these curves are quite similar to the curve of $\zeta_\pi(T)$ at vanishing μ_B but their minima are only shifted towards lower T as μ_B increases. Following the same story of vanishing μ_B , inclusion of baryon loops in pion self-energy is again influencing on $\zeta_\pi(T)$ in high temperature domain. The variation with μ_B of $\zeta_N(\mu_B)$ in Fig. 6(a) and $\zeta_\pi(\mu_B)$ in Fig. 6(b) and (c) are grossly same as their temperature dependence. For small T and μ_B , ζ_N and ζ_π are of similar order. However, with increasing T and μ_B , ζ_N dominates over ζ_π . ζ_N receives additional contribution from $\left(\frac{\partial P}{\partial \rho_B}\right)_\epsilon$. One should keep in mind that the term $\left(\frac{\partial P}{\partial \rho_B}\right)_\epsilon$ goes to zero for $\mu_B = 0$. The T and μ_B dependence of $\left(\frac{\partial P}{\partial \rho_B}\right)_\epsilon$ are shown in Fig. 7(b) and (d)

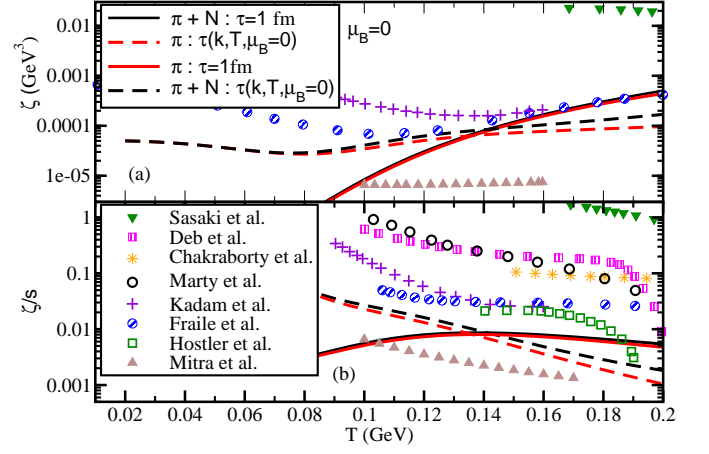


FIG. 11: (Color online) Our results of ζ (a) and ζ/s (b) vs T at $\mu_B = 0$ are compared with the earlier results of Sasaki et al. (Green triangles down [20]), Deb et al. (Pink solid squares [25]), Chakraborty et al. (Brown stars [28]), Marty et al. (open circles [21]), Kadam et al. (Violet pluses [34]), Fraile et al. (Blue solid circles), Hostler et al. (Open squares [36])

respectively while Fig. 7(a) and (c) are displaying the T and μ_B dependence of c_s^2 . From Fig. 7(a), we see that our $c_s^2(T, \mu_B = 0)$ curve (solid line) is in good agreement with LQCD results [3] (circles) within the hadronic temperature domain ($T < 0.160$ GeV). Total bulk viscosity ζ_T (a), entropy density s (b) and their ratio ζ/s (c) are plotted against T in Fig. (8) and μ_B in Fig. (9) at three different values μ_B and T respectively. Since increment of $s(T)$ is larger than the increment of $\zeta(T)$, therefore, ζ/s is appeared as a decreasing function of T . On the other hand, both $\zeta(\mu_B)$ and $s(\mu_B)$ monotonically increase with μ_B but the ratio $\zeta/s(\mu_B)$ increases first and then decreases at high μ_B domain. Next, Fig. 10(a), (b) and (c) reveal respectively the variation of total bulk viscosity ζ , entropy density s and their ratio with the variation of center of mass energy \sqrt{s} (Reader are requested to be careful on the same symbol s used for entropy density and square of beam energy). The beam energy dependence of T and μ_B used in computation are those obtained from fits to hadron yields. We have used the parameterization from Ref. [48]. We notice in Fig. 10 that ζ (a) as well as ζ/s (c) are decreasing with \sqrt{s} , which is qualitatively agreeing with the results of earlier studies [33, 34]. The decreasing trend of ζ and ζ/s with \sqrt{s} can be understood from the fact that μ_B decreases with \sqrt{s} while T remains fairly constant in the range of \sqrt{s} analyzed here and according to Fig. 9(a) and (c), the ζ and ζ/s decreases with decreasing of μ_B .

Fig. 11 is dedicated for comparative understanding of our results with respect to the earlier investigations. As most of the works have been done at $\mu_B = 0$, so we have plotted ζ (a) and ζ/s (b) against T for $\mu_B = 0$, where our results for π - component (red lines) and $(\pi + N)$ - components (black lines), using our calculated $\tau(\vec{k}, T, \mu_B = 0)$

(dashed lines) and constant τ (solid lines), are compared with the results, obtained by Sasaki et al. (Green triangles down [20]), Deb et al. (Pink solid squares [25]), Chakraborty et al. (Brown stars [28]), Marty et al. (open circles [21]), Kadam et al. (Violet pluses [34]), Fraile et al. (Blue solid circles), Hostler et al. (Open squares [36]). We see a large numerical band for ζ (10^{-5} - 10^{-2} GeV³) or ζ/s (10^{-3} - 10^0), within which earlier estimations are located. The results of the present work and Fraile et al. [37] both show similar kind of temperature dependence of ζ - it decreases at low T domain (< 0.100 GeV) and then increases at high T domain (> 0.100 GeV). Monotonically increasing nature of $\zeta(T)$ for constant value of τ (solid lines) discloses the fact that the origin of non-monotonic behavior of dashed lines are because of explicit structure of $\tau(\vec{k}, T, \mu_B = 0)$. The $\zeta(T)$ of Ref. [34] decreases up to $T \sim 0.150$ GeV after which a mild increment is observed. Most of the earlier works [20, 21, 25, 27, 28, 32, 34–37] based on effective QCD model calculations [20, 21, 25, 27, 28] as well as effective hadronic model calculations [32, 34–37] predicted a decreasing function of $\zeta/s(T)$ in the hadronic temperature domain, which is qualitatively similar with our results (dashed lines). These are not supporting the fact that ζ/s diverges or becomes large near the transition temperature as indicated by Refs. [2, 4, 5], within the temperature domain of quark phase. Some of the effective QCD model calculations [22–24, 27], which can predict estimations of ζ/s in both temperature domain, exposed a peak structure near the transition temperature. While some of the HRG model calculations [33, 36] have supported this behavior by displaying an increasing tendency of $\zeta/s(T)$ as one goes towards the transition temperature from the hadronic temperature domain. This kind of increasing $\zeta/s(T)$ is also observed in our work when we consider the constant value of τ (solid lines). Regarding this two opposite nature of $\zeta/s(T, \mu_B = 0)$ within hadronic temperature domain, Ref. [27, 36] have exposed the possibility of both nature. Ref. [36] shows that inclusion Hagedorn states (HS) in HRG model can convert $\zeta/s(T)$ from decreasing to increasing function. In this context, our results for explicit T, μ_B dependent τ and constant value of τ are also displaying both type of nature. Taking shear viscosity $\eta(T, \mu_B = 0)$ from Ref. [45], based on same pion and nucleon thermal fluctuations, we get $\zeta/\{(1/3 - c_S^2)^2\eta\} \approx 5 - 4$ and $\zeta/\{(1/3 - c_S^2)\eta\} \approx 0.8 - 0.7$. This is supporting the estimation of gravity dual theory [49] instead of the relation $\zeta/\{(1/3 - c_S^2)^2\eta\} \approx 15$, followed by photon fields [50], scalar fields [51] or QCD theory [19]. So our estimation within the hadronic temperature domain is representing the strongly coupled picture instead of weakly coupled scenario [19]. Again, at high temperature domain, our numerical values of ζ/s are matching (after extrapolation) with high temperature values of Refs. [19, 52]- $\zeta/s(T \approx 0.200 - 0.400) \approx 0.002 - 0.001$, obtained from the perturbative QCD calculations. In this regard, our estimation is indicating a smooth transformation from

the strongly coupled picture of the hadronic temperature domain to a weakly coupled medium of quarks, instead of divergence or peak structure of ζ/s near transition temperature.

IV. SUMMARY

We have gone through a detailed microscopic calculation of bulk viscosity coefficient for hadronic matter, where thermodynamical equilibrium conditions of all hadrons in medium have been treated by standard HRG model, which is very successful to generate LQCD thermodynamics up to the transition temperature. The thermal widths of medium constituents in the bulk viscosity expression inversely determine their numerical strength. Assuming pions and nucleons as most abundant medium constituents, we have concentrated on the bulk viscosity contributions from pion and nucleon components, where their corresponding thermal widths are derived from their in-medium scattering probabilities with different mesonic and baryonic resonances in the hadronic matter. Owing to the field theory version of optical theorem, the imaginary part of pion and nucleon self-energy (on-shell) at finite temperature give the estimation of their corresponding thermal widths. In the one-loop diagrams of pion self-energy, we have taken different mesonic and baryonic loops, while pion-baryon intermediate states are considered in the one-loop diagrams of nucleon self-energy. Their thermal widths are basically on-shell values of their corresponding Landau cut contributions, which disappear in the absence of medium and therefore, these are inversely interpreted as their respective relaxation time, which proportionally control the numerical strength of transport coefficients like ζ . Our result show that $\zeta(T)$ at $\mu_B = 0$ increases in the high temperature domain ($0.080 < T(\text{GeV}) < 0.175$) but a decreasing nature of $\zeta(T)$ has also been observed at low T (< 0.08 GeV). The $\pi\sigma$ and $\pi\rho$ loops of pion self-energy are respectively responsible for the decreasing and increasing nature of $\zeta(T)$ at low and high T domain. Addition of baryon loops in pion self-energy mainly make $\zeta(T)$ reduce at high T domain. Bulk viscosity for nucleon component monotonically increases with T . At finite μ_B , the nucleon component of bulk viscosity is highly dominating over the pion component. Adding nucleon and pion components, the total ζ increases with both T and μ_B . However, after dividing by total entropy density, ζ/s appear as a decreasing function of T and with the variation of μ_B , it increases first at low μ_B region and then decreases at high μ_B region. Along the beam energy axis, the ζ and ζ/s both decreases, as noticed in some earlier works [33–35].

During comparison with earlier results of $\zeta/s(T)$ at $\mu_B = 0$, one can notice that the qualitative as well as quantitative nature is not a very settled issue. Some of them [2, 4, 5] indicated divergence tendency of ζ/s near transition temperature, some of effective QCD model cal-

culations [22–24, 27] revealed peak structure near transition temperature, whereas most of the effective QCD model calculations [20, 21, 25, 27, 28] as well as effective hadronic model calculations [32, 34–37], including our present work, predict a decreasing function of $\zeta/s(T)$ in the hadronic temperature domain, with few exceptional HRG calculations [33, 36]. Our decreasing $\zeta/s(T, \mu_B = 0)$ is representing a strongly coupled picture in the hadronic temperature domain, whose smooth extrapolation to high temperature domain agrees with a weakly coupled picture [19].

Acknowledgment : During first and major part of this work, SG is financially supported by the DST project with no NISER/R&D-34/DST/PH1002, (with title “*Study of QCD phase Structure through high en-*

ergy heavy ion collisions” and principal investigator Prof. B. Mohanty). During the last part of the work, SG is supported from UGC Dr. D. S. Kothari Post Doctoral Fellowship under grant No. F.4-2/2006 (BSR)/PH/15-16/0060. SC acknowledges XIIth plan project no. 12-R&D-NIS-5.11-0300 and CNT project PIC XII-R&D-VECC-5.02.0500 for support. SG thanks to high energy group of NISER (Prof. B. Mohanty, Dr. A. Das, Dr. C. Jena, Dr. R. Singh, R. Haque, V. Bairathi, K. Nayak, V. Lyar, S. Kundu and others) and group of Calcutta University (Prof. A. Bhattacharyya, Prof. G. Gangopadhyay) for getting various academic and non-academic support at NISER and CU during this work and also to Dr. V. Roy and Prof. H. Mishra for some discussion regarding this work.

-
- [1] P. Kovtun, D. T. Son, and O. A. Starinets, Phys. Rev. Lett. **94**, 111601 (2005).
 - [2] D. Kharzeev and K. Tuchin, J. High Energy Phys. **09** (2008) 093
 - [3] A. Bazavov *et al.* (HotQCD Collaboration), Phys. Rev. D **90**, 094503 (2014).
 - [4] H. B. Meyer, Phys. Rev. Lett. **100**, 162001 (2008)
 - [5] F. Karsch, D. Kharzeev, and K. Tuchin, Phys. Lett. B **663**, 217 (2008).
 - [6] G. Torrieri and I. Mishustin, Phys. Rev. C **78**, 021901 (2008).
 - [7] A. Monnai and T. Hirano, Phys. Rev. C **80**, 054906 (2009).
 - [8] G. S. Denicol, T. Kodama, T. Koide and P. Mota, Phys. Rev. C **80**, 064901 (2009).
 - [9] K. Rajagopal and N. Tripuraneni, JHEP **1003**, 018 (2010).
 - [10] P. Bozek, Phys. Rev. C **81**, 034909 (2010); Phys. Rev. C **85**, 034901 (2012); P. Bozek and I. Wyskiel-Piekarska, Phys. Rev. C **85**, 064915 (2012).
 - [11] H. Song and U. W. Heinz, Phys. Rev. C **81**, 024905 (2010).
 - [12] J. Bhatt, H. Mishra, V. Sreekanth, J. High Energy Phys. **1011** (2010) 106; Phys. Lett. B **704** (2011) 486; Nucl. Phys. A **875** (2012) 181.
 - [13] K. Dusling and T. Schfer, Phys. Rev. C **85**, 044909 (2012).
 - [14] V. Roy and A.K. Chaudhuri, Phys. Rev. C **85** (2012) 024909.
 - [15] J. Noronha-Hostler, G. S. Denicol, J. Noronha, R. P. G. Andrade and F. Grassi, Phys. Rev. C **88**, 044916 (2013).
 - [16] J. Noronha-Hostler, J. Noronha and F. Grassi, Phys. Rev. C **90**, no. 3, 034907 (2014).
 - [17] M. Habich and P. Romatschke, JHEP **12** (2014) 054.
 - [18] S. Ryu, J.F. Paquet, C. Shen, G.S. Denicol, B. Schenke, S. Jeon, C. Gale, Phys. Rev. Lett. **115** (2015) no.13, 132301
 - [19] P. Arnold, C. Dogan, G. D. Moore, Phys. Rev. D **74**, 085021 (2006).
 - [20] C. Sasaki and K. Redlich, Phys. Rev. C **79**, 055207 (2009); Nucl. Phys. A **832** (2010) 62.
 - [21] R. Marty, E. Bratkovskaya, W. Cassing, J. Aichelin, H. Berrehrah Phys. Rev. C **88** (2013) 045204.
 - [22] S. Xiao, L. Zhang, P. Guo, D. Hou, Chin. Phys. C **38** (2014) 054101.
 - [23] S. Ghosh, T. C. Peixoto, V. Roy, F. E. Serna, G. Krein, Phys. Rev. C **93** (2016) 045205.
 - [24] K. Saha and S. Upadhaya, arXiv:1505.00177 [hep-ph].
 - [25] P. Deb, G. Kadam, H. Mishra, arXiv:1603.01952 [hep-ph].
 - [26] K. Paech and S. Pratt, Phys. Rev. C **74**, 014901 (2006).
 - [27] A. Dobado and J. Torres Rincon, Phys. Rev. D **86**, 074021 (2012); A. Dobado, F.J. Llanes-Estrada, J. Torres Rincon, Phys. Lett. B **702**, 43 (2011).
 - [28] P. Chakraborty and J. I. Kapusta, Phys. Rev. C **83**, 014906 (2011).
 - [29] V. Chandra, Phys. Rev. D **84**, 094025 (2011); Phys. Rev. D **86**, 114008 (2012).
 - [30] S. K. Das, J. Alam Phys. Rev. D **82** (2010) 051502.
 - [31] Gavin, S. Nucl. Phys. A **435** (1985) 826.
 - [32] S. Mitra and S. Sarkar, Phys. Rev. D **87**, 094026 (2013); S. Mitra, S. Gangopadhyaya, and S. Sarkar, Phys. Rev. D **91**, 094012 (2015)
 - [33] G. P. Kadam, H. Mishra, Nucl. Phys. A **934** (2014) 133.
 - [34] G. P. Kadam, H. Mishra, Phys. Rev. C **92** (2015) 035203; Phys. Rev. C **93** (2016) 025205.
 - [35] G. Sarwar, S. Chatterjee, J. Alam arXiv: 1512.06496[nucl-th].
 - [36] J. Noronha-Hostler, J. Noronha and C. Greiner, Phys. Rev. Lett. **103**, 172302 (2009).
 - [37] D. Fernandez-Fraile and A. Gomez Nicola, Eur. Phys. J. C **62**, 37 (2009); Phys. Rev. Lett. **102**, 121601 (2009).
 - [38] K.A. Olive *et al.* (Particle Data Group), Chin. Phys. C, **38**, 090001 (2014).
 - [39] A. Bazavov, T. Bhattacharya, M. Cheng, *et al.*, Phys. Rev. D **80**, 014504 (2009).
 - [40] S. Borsanyi *et al.*, J. High. Ener. Phys. **1009**, 73 (2010).
 - [41] S. Borsanyi, Z. Fodor, S. D. Katz, S. Krieg, C. Ratti, and K. Szabo, J. High. Ener. Phys. **1201**, 138 (2012).
 - [42] S. Ghosh, G. Krein, S. Sarkar, Phys. Rev. C **89** (2014) 045201.
 - [43] M. Post, S. Leupold, U. Mosel, Nucl. Phys. A **741**, 81 (2004).
 - [44] S. Ghosh, J. Phys. G **41**, 095102 (2014).
 - [45] S. Ghosh, Braz. J. Phys. **45** (2015) 687.
 - [46] S. Ghosh, Phys. Rev. C **90**, 025202 (2014).

- [47] S. Ghosh, Braz. J. Phys. 44, 789 (2014).
- [48] F. Karsch and K. Redlich, Phys. Lett. **B 695**, 136-142 (2011)
- [49] P. Benincasa, A. Buchel, and A. O. Starinets, Nucl. Phys. **B 733**, 160 (2006); A. Buchel, Phys. Rev. D 72, 106002 (2005).
- [50] S. Weinberg, Astrophys. J. 168, 175 (1971).
- [51] R. Horsley and W. Schoenmaker, Nucl. Phys. **B 280**, 716 (1987).
- [52] J. I. Kapusta, *Relativistic Nuclear Collisions*, Landolt-Bornstein New Series, Vol. I/23, ed. R. Stock (Springer-Verlag, Berlin Heidelberg 2010); L. P. Csernai, J. I. Kapusta, and L. D. McLerran, Phys. Rev. Lett. **97**, 152303 (2006).